Experimental Investigation of State Distinguishability in Parity-Time Symmetric Quantum Dynamics

Yi-Tao Wang, Zhi-Peng Li, Shang Yu, Zhi-Jin Ke, Wei Liu, Yu Meng, Yuan-Ze Yang, Jian-Shun Tang,* Chuan-Feng Li,† and Guang-Can Guo

CAS Key Laboratory of Quantum Information, University of Science and Technology of China, Hefei 230026, People's Republic of China

and CAS Center For Excellence in Quantum Information and Quantum Physics, University of Science and Technology of China, Hefei 230026, People's Republic of China

(Received 20 October 2019; accepted 26 May 2020; published 11 June 2020)

Comprehensive study on parity-time ($\mathcal{PT}$) symmetric systems demonstrates the novel properties and innovative application of non-Hermitian physics in recent years. In the quantum regime, $\mathcal{PT}$ symmetric physics exhibits unique quantum dynamical behaviors such as spontaneous state-distinguishability oscillation. However, the construction and control of a $\mathcal{PT}$ symmetric quantum system are still challenging, that and restrict the experimental investigation of $\mathcal{PT}$ symmetric quantum nature and application. In this Letter, we propose and construct a recycling-structure $\mathcal{PT}$ symmetric quantum simulator for the first time, which can effectively simulate the discrete-time dynamical process of a $\mathcal{PT}$ symmetric quantum system in both unbroken and broken phases, to be different from our previous work [J.-S. Tang, et al., Nat. Photonics 10, 642 (2016)]. We investigate the dynamical features of quantum state distinguishability based on the $\mathcal{PT}$ symmetric simulator. Our results demonstrate the novel $\mathcal{PT}$ symmetric quantum dynamics characterized by the periodical oscillation of state distinguishability in the unbroken phase, and the monotonic decay of that in the broken phase. This work also provides a practical experimental platform for the future intensive study of $\mathcal{PT}$ symmetric quantum dynamics.

DOI: 10.1103/PhysRevLett.124.230402

Introduction.—A Hamiltonian together with a dynamical equation, e.g., the Schrödinger equation in quantum mechanics, determine the performance of system dynamics, in which a Hermitian Hamiltonian featuring real eigenvalues guarantees the reality of system eigenenergies. As a class of special non-Hermitian Hamiltonian, the parity-time ($\mathcal{PT}$) symmetric Hamiltonian possesses the real eigenvalue spectrum and critical behaviors near an exceptional point [1,2], therefore, it characterizes a class of dynamical modes, which are absent in conventional Hermitian systems but emerge with novel features in $\mathcal{PT}$ symmetric systems [3]. Based on the fundamental structure of coupled gain and loss subsystems, $\mathcal{PT}$ symmetric dynamics has been observed in various classical systems, such as an optical waveguide [4,5], microwave waveguide [6], microcavity [7,8], metasurface [9], electronic circuit [10], atom-mediated optical system [11,12], and optically mediated mechanical system [13]. Taking advantage of the unique non-Hermitian properties, these $\mathcal{PT}$ symmetric systems are further developed as various functional devices [14,15], such as a high-sensitivity sensor [16], single-mode laser [17–19], nonreciprocal device [7,20], wireless power transfer [21], and topological mode transfer [6,13]. The intensive study of $\mathcal{PT}$ symmetric physics on the extensive classical systems has demonstrated the novel properties and outstanding applications of non-Hermitian physics.

Towards the quantum regime, the $\mathcal{PT}$ symmetric system also exhibits novel behaviors absent in the conventional quantum system. State distinguishability, i.e., capacity of two quantum states to be distinguished by quantum-mechanical measurement, was revealed oscillating spontaneously in the $\mathcal{PT}$ symmetric unbroken phase and decaying monotonically in the broken phase [22]. State distinguishability is a basic notion in quantum hypothesis testing and state discrimination [23], and utilized in many quantum-information applications such as quantum cryptography [24] and quantum non-Markovianity identification [25,26]. It should be non-increasing in the Hermitian system and Markovian system as a comparison to that in the $\mathcal{PT}$ symmetric system. The oscillation period and decay rate of state distinguishability can be controlled by a non-Hermitian degree in $\mathcal{PT}$ symmetric system, where the exceptional point corresponds to the phase transition criticality of the state-distinguishability dynamics. $\mathcal{PT}$ symmetric quantum dynamics possesses the unique properties which are completely distinct from the dynamical behaviors in conventional quantum systems such as the closed Hermitian system and open Markovian or non-Markovian system. Therefore, thorough experimental investigation is crucial for the deeper understanding of $\mathcal{PT}$-symmetry-induced state-distinguishability dynamics.

However, in contrast to classical systems, quantum-regime $\mathcal{PT}$ symmetric physics is still obscure on an

 © 2020 American Physical Society

experimental platform [3,15], since the full control of a $\mathcal{PT}$ symmetric quantum system is challenging. $\mathcal{PT}$-symmetric-Hamiltonian-driven dynamics has been observed in some quantum systems, e.g., light-matter quasiparticles [27], a cold atom [28], and the nitrogen-vacancy center in diamond [29], while the thorough experimental study of $\mathcal{PT}$ symmetric quantum properties and applications is the further goal to be achieved. On the other hand, quantum simulation is another effective route to access objective quantum behaviors [30,31]. In our previous work [32], a single $\mathcal{PT}$-symmetric quantum evolution was simulated in a single-photon system, but the simulation of $\mathcal{PT}$ symmetric quantum dynamics was unexplored.

In this Letter, we propose and construct the recycling-structure $\mathcal{PT}$ symmetric quantum simulator for the first time, which makes it possible to simulate the discrete-time $\mathcal{PT}$ symmetric quantum dynamics beyond the single evolution. Moreover, based on the quantum simulator, we observe the $\mathcal{PT}$ symmetric dynamics in both unbroken and broken phases. and investigate unique state-distinguishability dynamical behaviors. This work demonstrates the $\mathcal{PT}$-symmetric-Hamiltonian-induced periodical oscillation of state distinguishability in the $\mathcal{PT}$ symmetric unbroken phase and monotonic decay of that in the broken phase. The dynamics transition behaves as the characteristic-time criticality at the exceptional point. The work also provides and demonstrates a practical experimental platform of the $\mathcal{PT}$ symmetric quantum simulator for further study of non-Hermitian quantum physics.

Theory.—The two-level $\mathcal{PT}$ symmetric Hamiltonian investigated in our work can be written as

$$\boldsymbol{H} = \begin{pmatrix} ia & 1 \\ 1 & -ia \end{pmatrix}, \tag{1}$$

where the nonunit real parameter $a \geq 0$ represents the non-Hermitian degree. $a \in [0, 1)$, $a \in (1, +\infty)$, $a = 0$, and $a = 1$ correspond to the $\mathcal{PT}$ symmetric unbroken phase, $\mathcal{PT}$ symmetric broken phase, Hermitian point, and exceptional point, respectively. The nonunit $\mathcal{PT}$ symmetric evolution operator of time t can be deduced as

$$\boldsymbol{U}(t) = e^{-i\boldsymbol{H}t} = \frac{1}{\sqrt{1-a^2}} \begin{pmatrix} g_1 + g_2 & -i\sin\theta \\ -i\sin\theta & g_1 - g_2 \end{pmatrix}, \tag{2}$$

where $g_1 = \sqrt{1-a^2}\cos\theta$, $g_2 = a\sin\theta$, and $\theta = \sqrt{1-a^2}t$. We want to note that the actual Hamiltonian and evolution time for the actual physical system should be actually written as $\mathcal{H} = \epsilon_1 \boldsymbol{H}$ and $\mathcal{T} = \epsilon_2 t$ with units, respectively. The constants ϵ_1 and ϵ_2 with units are determined by the specific actual system, with the relation that $\epsilon_1\epsilon_2/\hbar$ is a nonunit constant. For simplicity and without loss of generality, the unit terms ϵ_1, ϵ_2, and $\hbar$ are left out here, and only the nonunit parts are considered below. The dynamical map of the $\mathcal{PT}$ symmetric system is given by

$$\xi[\boldsymbol{\rho}(0), t] = \frac{\boldsymbol{U}(t)\boldsymbol{\rho}(0)\boldsymbol{U}^\dagger(t)}{\mathrm{Tr}[\boldsymbol{U}(t)\boldsymbol{\rho}(0)\boldsymbol{U}^\dagger(t)]}, \tag{3}$$

and the quantum state evolving at time t is deduced as $\boldsymbol{\rho}(t) = \xi[\boldsymbol{\rho}(0), t]$. In general quantum systems, the trace distance represents the natural metric distance of two quantum states in the space of physical states [33], which is defined as

$$D[\boldsymbol{\rho}_1(t), \boldsymbol{\rho}_2(t)] = \frac{1}{2}\mathrm{Tr}|\boldsymbol{\rho}_1(t) - \boldsymbol{\rho}_2(t)|, \tag{4}$$

where $|\boldsymbol{A}| = \sqrt{\boldsymbol{A}^\dagger\boldsymbol{A}}$, $\boldsymbol{\rho}_1(t)$ and $\boldsymbol{\rho}_2(t)$ are the density matrices of the two states. Trace distance $D[\boldsymbol{\rho}_1(t), \boldsymbol{\rho}_2(t)] \in [0, 1]$, and has the following physical properties: (1) It is invariant under unitary transformations and nonincreasing under completely positive and trace-preserving (CPTP) maps [34,35]; (2) It can be physically interpreted as the distinguishability of the two quantum states, since $\{1 + D[\boldsymbol{\rho}_1(t), \boldsymbol{\rho}_2(t)]\}/2$ is the maximal probability to discriminate the correct states when the two states are prepared beforehand with the probability $1/2$ for each other to be discriminated [24,36]. Therefore, the trace distance of Eq. (4) is an effective measure to quantify the state distinguishability in quantum dynamics [22,24].

Experiment.—The principal frameworks of quantum simulation schemes are shown in Fig. 1. The general quantum simulator is characterized by a black box in Fig. 1(a), which operates to map the arbitrary input state $\boldsymbol{\rho}(0)$ to the evolved state $\tilde{\boldsymbol{\rho}}(t)$ by the simulated dynamical map $\tilde{\xi}$ functioning as $\tilde{\boldsymbol{\rho}}(t) = \tilde{\xi}[\boldsymbol{\rho}(0), t]$. The simulation ability can be embodied as $\tilde{\boldsymbol{\rho}}(t) \approx \xi[\boldsymbol{\rho}(0), t]$, where t is the objective evolution time deduced from the simulation setting. The dynamical process can be determined by detecting and collecting the evolved states over time. According to Eq. (3), it is clear that the $\mathcal{PT}$ symmetric dynamical map is P divisible. Therefore, the quantum simulator can be disassembled as the chain structure in the discrete-time mode shown in Fig. 1(b), which is constituted by the uniform quantum gates operating as $\tilde{\boldsymbol{U}}$. $\tilde{\boldsymbol{U}}$ possesses

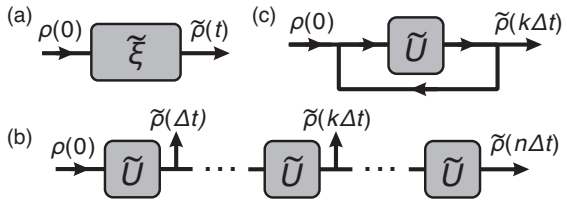

FIG. 1. Principal framework of three types of quantum simulations. (a) General quantum simulation, operating as the dynamical map $\tilde{\boldsymbol{\rho}}(t) = \tilde{\xi}[\boldsymbol{\rho}(0), t]$. (b) Chain-structure quantum simulation, outputting the dynamical process of $0 - n$ steps with the discrete time of Δt. (c) Recycling-structure quantum simulation, reducing the construction complexity by recycling the quantum objective.

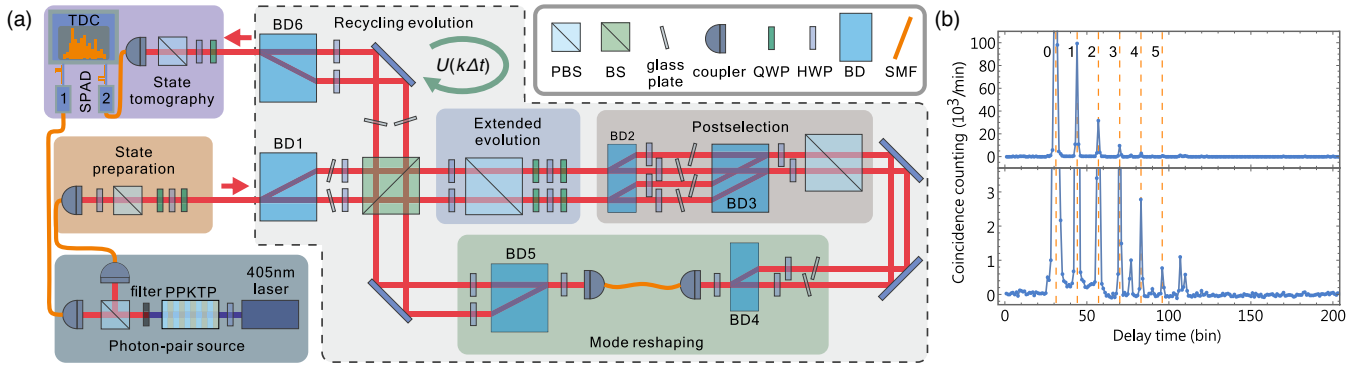

FIG. 2. (a) Experimental setup of the recycling-structure $\mathcal{PT}$ symmetric quantum simulator. (b) Background-noise-subtracted coincidence-counting spectrum (top) and the corresponding part-enlarged spectrum (bottom). The delay time is the time interval between the trigger and target photons, discretized by the 648-ps-width TDC time bin. The orange dashed lines indicate the coincidence signals of recycling rounds 0–5, where the adjacent-signal interval is 13 bins. PBS, polarizing beam splitter; BS, beam splitter; QWP, quarter-wave plate; HWP, half-wave plate; BD, beam displacer; SMF, single-mode fiber; PPKTP, periodically poled potassium titanyl phosphate; SPAD, single-photon avalanche diode; TDC, time-digital converter.

the effective simulation as the evolution $\boldsymbol{U}(\Delta t)$, where Δt is the discrete evolution time. Furthermore, the recycling scheme can be applied to reduce the complexity of the quantum-gate construction, and the recycling-structure quantum simulator is shown in Fig. 1(c), where the discrete-time quantum dynamical process is obtained by collecting the evolved states during successive-round recycling operation. The $\mathcal{PT}$ symmetric quantum simulator in our work is built using the method of recycling-structure simulation, which is constituted by the quantum gate simulating two-level $\mathcal{PT}$ symmetric evolution. The quantum gate is constructed based on a sequence of operations on the quantum space with extended dimensions of a single photon, and the simulated $\mathcal{PT}$ symmetric system is obtained effectively by performing appropriate projection measurement on the ancilla space of the single photon.

The experimental setup of the recycling-structure $\mathcal{PT}$ symmetric quantum simulator is shown in Fig. 2(a), which is constituted by four modules: (1) Photon-pair source. It generates the target photon and trigger photon simultaneously by spontaneous parametric down conversion. The former is set as the qubit carrier for the following simulation operation, and the latter is detected directly as the trigger signal, which can be used as the time stamp marking different recycling rounds and substantially reduce the detecting noise. (2) State preparation. The polarization state of the target photon is prepared to the desired initial state in this module. (3) Recycling evolution. This module applies extended evolution, postselection, and mode reshaping on the target photon in the recycling loop successively, to realize an effective quantum gate of $\mathcal{PT}$ symmetric evolution. The photon is output from the loop with certain probability (set as $1/2$ here), or reflected by the beam splitter (BS) to be recycled for the next-round evolution. (4) State tomography. The density matrix of the output-photon polarization state is acquired, after the coincidence-counting spectrum of photon pairs at different delay times is recorded in this module. One of the typical background-noise-subtracted spectra is shown in Fig. 2(b) [37]. The orange dashed lines in Fig. 2(b) indicate the coincidence signals from the photon pairs with time stamps of $k = 0 \sim 5$, which mark the signals corresponding to the discrete-time dynamical process with successive-round evolution. The simulated evolution time is deduced by $t = k\Delta t$, where Δt is the single-round evolution time set by extended evolution in module (3).

In the recycling evolution module, the polarization state (path state) is transferred to the path state (polarization state) by beam displacer BD1 (BD6) together with half-wave plates at the entrance (exit) of the recycling loop. Extended evolution and postselection are applied on the extended quantum space, to realize the effective $\mathcal{PT}$ symmetric evolution on the one-qubit system. The state input into extended evolution for the kth evolution is set as

$$|\psi_{k-1}\rangle = |H\rangle|\phi_{k-1}\rangle, \tag{5}$$

where the path state $|\phi_{k-1}\rangle = \alpha_{k-1}|U\rangle + \beta_{k-1}|D\rangle$, with α_{k-1} and β_{k-1} are the complex coefficients, $|U\rangle$, $|D\rangle$ and $|H\rangle$ are the up-path, down-path, and horizontal-polarization states, respectively. The normalization coefficient is omitted here and below for simplicity. The state output from extended evolution is $\alpha_{k-1}|U\rangle\boldsymbol{U}(\Delta t)|H\rangle + \beta_{k-1}|D\rangle\boldsymbol{U}(\Delta t)|V\rangle$, where $|V\rangle$ is the vertical-polarization state. By taking the polarization qubit as the ancilla in postselection and performing a projection measurement on the superposition state $(|H\rangle + |V\rangle)/\sqrt{2}$ of ancilla, the state output from postselection is $|H\rangle(\alpha_k|U\rangle + \beta_k|D\rangle)$, where $\alpha_k = \alpha_{k-1}\langle H|\boldsymbol{U}(\Delta t)|H\rangle + \beta_{k-1}\langle H|\boldsymbol{U}(\Delta t)|V\rangle$ and $\beta_k = \alpha_{k-1}\langle V|\boldsymbol{U}(\Delta t)|H\rangle + \beta_{k-1}\langle V|\boldsymbol{U}(\Delta t)|V\rangle$. In a word, extended evolution and postselection operate as the iterative map to output the state through the kth-round evolution:

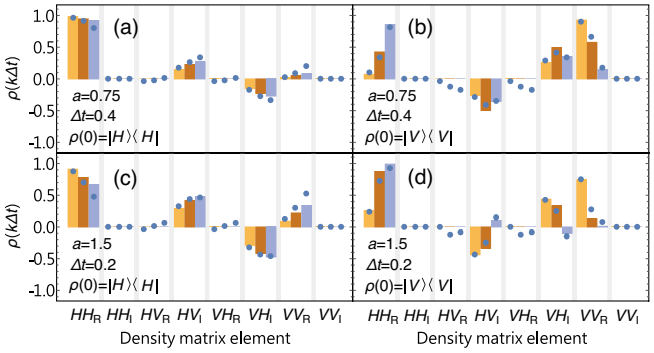

FIG. 3. Density matrices of the evolved states during three-round recycling evolutions output from the simulator. (a),(b) Results in $\mathcal{PT}$ symmetric unbroken phase. (c),(d) Results in $\mathcal{PT}$ symmetric broken phase. Density matrix elements XY_{R} and XY_{I} represent the matrix elements of $\mathrm{Re}(\langle X|\rho(k\Delta t)|Y\rangle)$ and $\mathrm{Im}(\langle X|\rho(k\Delta t)|Y\rangle)$, respectively. For every matrix element, the successive three results correspond to evolved state $\rho(k\Delta t)$ with $k = 1 \sim 3$. The histograms and points indicate the theoretical and experimental results, respectively. The parameters of non-Hermitian degree a, single-round evolution time Δt, and initial state $\rho(0)$ are marked in (a)–(d).

$$|\psi_k\rangle = |H\rangle \boldsymbol{U}(\Delta t)|\phi_{k-1}\rangle. \tag{6}$$

Mode reshaping in module (3) operates to renormalize the beam size by coupling the beam into the single-mode fiber, preventing considerable beam expansion during propagation in the recycling loop. More details of the experimental setup and methods are referred to in the Supplemental Material [37].

Results.—The density matrices of the output states during three-round iterative evolution are shown in Fig. 3, with the initial states set to $|H\rangle$ and $|V\rangle$. The density-matrix elements in the $\mathcal{PT}$ symmetric unbroken phase are shown in Figs. 3(a) and 3(b) with the non-Hermitian degree $a = 0.75$ and single-round evolution time $\Delta t = 0.4$, and those in broken phase are shown in Figs. 3(c) and 3(d) with $a = 1.5$ and $\Delta t = 0.2$. The evolved states corresponding to more rounds are not taken into account since their signals are too weak and overwhelmed by noise in some measurement bases. To acquire the states during longer evolution time, the initial states are renormalized as the final states output from the last-round evolution, and are input into the recycling evolution module for the following-round evolution. The whole dynamical process is obtained by this iterative method for the following investigation of state-distinguishability dynamics.

The dynamics of state distinguishability in the $\mathcal{PT}$ symmetric quantum system is shown in Fig. 4, where the points are the experimental results acquired from the simulator, and the lines are the corresponding theoretical results. The state-distinguishability dynamical behaviors are indicated by the evolution of trace distance defined as Eq. (4), with $|H\rangle$ and $|V\rangle$ being the two orthogonal initial states. The state distinguishability is invariant and equals to

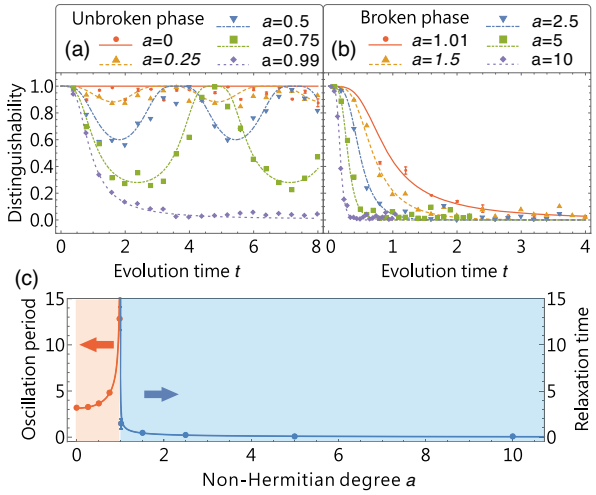

FIG. 4. State-distinguishability dynamics in $\mathcal{PT}$ symmetric (a) unbroken and (b) broken phase. The non-Hermitian degree a of all results are marked in figures. (c) Phase-transition process exhibited by the characteristic times of state-distinguishability dynamics, i.e., the oscillation period in unbroken phase (in the left orange region with $0 \leq a < 1$) and relaxation time in broken phase (in the right blue region with $a > 1$). The lines and points are theoretical and experimental results, respectively. Note that the units for the simulated time, including evolution time t, oscillation period, and relaxation time, are omitted here as discussed above, and their counterparts in real physical systems should include units determined by specific systems.

1 in the Hermitian system, as the results shown in Fig. 4(a) with $a = 0$. In the $\mathcal{PT}$ symmetric unbroken phase, the state distinguishability possesses remarkable periodic oscillation behavior shown in Fig. 4(a) with $a \neq 0$, which can fully recover in every period. The period increases with non-Hermitian degree, indicating that non-Hermitian degree can be developed as a parameter to control the quantum distinguishability. In the $\mathcal{PT}$ symmetric broken phase, the state distinguishability decays monotonically and the distinguishability-oscillation behavior disappears as shown in Fig. 4(b). The decay rate increases with non-Hermitian degree. The exceptional point corresponds to the state-distinguishability dynamical criticality as that shown in Fig. 4(c). The characteristic times of state-distinguishability dynamics are the oscillation period in the unbroken phase and the relaxation time in the broken phase, respectively. Both the characteristic times approach infinity near the exceptional point, exhibiting the phase-transition process of state distinguishability dynamics controlled by the $\mathcal{PT}$ symmetric phase.

Discussion and conclusion.—The quantum dynamics characterized by varying state distinguishability also exists in conventional open quantum systems, where the state-distinguishability increase is the indicator of non-Markovian quantum dynamics [25,26]. It should be noted that the non-Markovian quantum dynamics is completely distinct from the $\mathcal{PT}$ symmetric dynamics investigated in

this work. For non-Markovian dynamics, the dynamical maps can not be P divisible by definition. The objective non-Markovian system to be studied is concentrated on the linear quantum system, and the dynamical maps are CPTP maps for physical conditions. For $\mathcal{PT}$ symmetric dynamics, the dynamical maps are P divisible, and generally not trace-preserving. The state-distinguishability oscillation in $\mathcal{PT}$ symmetric dynamics can be directly interpreted as the result of the dynamical overlap between the skew eigenstates in the $\mathcal{PT}$ symmetric system, which is a remarkable characteristic absent in conventional open quantum systems [37]. In the unbroken phase, the overlap is nontrivial and generates a beat from the two skew dynamical eigenstates, where the beat period equals the oscillation period. In the broken phase, the overlap becomes trivial, and moreover, the amplitudes of the eigenstates grow or shrink monotonically under dynamical evolution, resulting in the state distinguishability decreasing monotonically [37].

To explain the intrinsic distinction between the $\mathcal{PT}$ symmetric quantum dynamics and conventional quantum dynamics, the fundamental physical interpretation of $\mathcal{PT}$ symmetric quantum mechanics can be established in two ways. One way is to redefine the inner product of the Hilbert space corresponding to the $\mathcal{PT}$ symmetric system [2], which could lead to the physical systems with a special metric operator and the application to deal with some problems in quantum cosmology [42,43]. The novel $\mathcal{PT}$ symmetric dynamics could be connected to the space metric transformation of the $\mathcal{PT}$ symmetric systems [44]. The other way is to treat the $\mathcal{PT}$ symmetric space as a projective space of an extended Hermitian space [44], which could lead to the design of larger Hermitian systems with different structures and projection methods. The $\mathcal{PT}$ symmetric dynamics could be explained by special designs like ancilla postselection [22,45] or weak measurement [31].

Besides the theoretical models established to explain the unique $\mathcal{PT}$ symmetric dynamics, the theoretical study for the quantum-information applications based on the unique $\mathcal{PT}$ symmetric state distinguishability may be required, since state distinguishability plays a very important role in many quantum information tasks [23–25] as mentioned in the *Introduction*. The recycling framework with state distinguishability demonstrated in this work could be directly developed and adapted for the related studies in the future.

It is worth noting that the method of the recycling-structure simulator shown in Fig. 2(a) is valid for arbitrary non-Hermitian evolution actually, but not restricted to $\mathcal{PT}$ symmetry [37]. Therefore, the recycling-structure quantum simulator demonstrated in this work can be extended directly to the simulation work for other non-Hermitian quantum dynamics like anti-$\mathcal{PT}$ symmetric dynamics [46] and pseudo-Hermitian dynamics [44,47], etc. Moreover, further improvement could be concentrated on the simulation of time-dependent non-Hermitian quantum dynamics, which could be realized by using a pulsed photon source and replacing some wave plates with temporally controlled electro-optical modulators in the recycling-structure simulator [37,48]. This improvement could make it possible to investigate the quantum topological switch encircling the exceptional point, which possesses great potential for a new method of quantum control [6].

In conclusion, we propose and construct a recycling-structure $\mathcal{PT}$ symmetric quantum simulator in discrete-time mode for the first time. The discrete-time quantum dynamical process of the single photon can be simulated effectively in both $\mathcal{PT}$ symmetric unbroken and broken phases. Based on this experimental platform, the $\mathcal{PT}$ symmetric state-distinguishability dynamical behaviors are investigated experimentally. It demonstrates the novel state-distinguishability-oscillation behavior in the $\mathcal{PT}$ symmetric unbroken phase, which is completely different from the conventional non-Markovian quantum dynamics. As a contrast, we also demonstrate the monotonic state-distinguishability decay in a $\mathcal{PT}$ symmetric broken phase. The results exhibit that the non-Hermitian degree characterizes the state-distinguishability criticality at the exceptional point. Our work provides a practical experimental platform for the investigation of the $\mathcal{PT}$ symmetric physics, and sheds light on the study of non-Hermitian properties and applications towards the quantum regime.

This work is supported by the National Key Research and Development Program of China (No. 2017YFA0304100), the National Natural Science Foundation of China (Grants No. 61327901, No. 11674304, No. 11822408, No. 61490711, No. 11774335, No. 11821404, and No. 11904356), the Key Research Program of Frontier Sciences of the Chinese Academy of Sciences (Grant No. QYZDY-SSW-SLH003), Fok Ying-Tong Education Foundation (No. 171007), the Youth Innovation Promotion Association of Chinese Academy of Sciences (Grant No. 2017492), the Foundation for Scientific Instrument and Equipment Development of Chinese Academy of Sciences (Grant No. YJKYYQ20170032), Science Foundation of the CAS (Grant No. ZDRW-XH-2019-1), Anhui Initiative in Quantum Information Technologies (AHY020100, AHY060300), the National Postdoctoral Program for Innovative Talents (Grant No. BX20180293), China Postdoctoral Science Foundation (Grant No. 2018M640587), the Fundamental Research Funds for the Central Universities (No. WK2470000026, No. WK2030000008 and No. WK2470000028).

Y.-T. W. and Z.-P. L. contributed equally to this work.

*tjs@ustc.edu.cn
†cfli@ustc.edu.cn

[1] C. M. Bender and S. Boettcher, Real Spectra in non-Hermitian Hamiltonians Having PT Symmetry, Phys. Rev. Lett. **80**, 5243 (1998).

[2] C. M. Bender, D. C. Brody, and H. F. Jones, Complex Extension of Quantum Mechanics, Phys. Rev. Lett. **89**, 270401 (2002).
[3] R. El-Ganainy, K. G. Makris, M. Khajavikhan, Z. H. Musslimani, S. Rotter, and D. N. Christodoulides, Non-Hermitian physics and PT symmetry, Nat. Phys. **14**, 11 (2018).
[4] A. Guo, G. J. Salamo, D. Duchesne, R. Morandotti, M. Volatier-Ravat, V. Aimez, G. A. Siviloglou, and D. N. Christodoulides, Observation of PT-Symmetry Breaking in Complex Optical Potentials, Phys. Rev. Lett. **103**, 093902 (2009).
[5] C. E. Rüter, K. G. Makris, R. El-Ganainy, D. N. Christodoulides, M. Segev, and D. Kip, Observation of parity-time symmetry in optics, Nat. Phys. **6**, 192 (2010).
[6] J. Doppler, A. A. Mailybaev, J. Böhm, U. Kuhl, A. Girschik, F. Libisch, T. J. Milburn, P. Rabl, N. Moiseyev, and S. Rotter, Dynamically encircling an exceptional point for asymmetric mode switching, Nature (London) **537**, 76 (2016).
[7] B. Peng, Ş. K. Özdemir, F. Lei, F. Monifi, M. Gianfreda, G. Lu Long, S. Fan, F. Nori, C. M. Bender, and L. Yang, Parity-time-symmetric whispering-gallery microcavities, Nat. Phys. **10**, 394 (2014).
[8] L. Chang, X. Jiang, S. Hua, C. Yang, J. Wen, L. Jiang, G. Li, G. Wang, and M. Xiao, Paritytime symmetry and variable optical isolation in activepassive-coupled microresonators, Nat. Photonics **8**, 524 (2014).
[9] M. Lawrence, N. Xu, X. Zhang, L. Cong, J. Han, W. Zhang, and S. Zhang, Manifestation of PT Symmetry Breaking in Polarization Space with Terahertz Metasurfaces, Phys. Rev. Lett. **113**, 093901 (2014).
[10] N. Bender, S. Factor, J. D. Bodyfelt, H. Ramezani, D. N. Christodoulides, F. M. Ellis, and T. Kottos, Observation of Asymmetric Transport in Structures with Active Nonlinearities, Phys. Rev. Lett. **110**, 234101 (2013).
[11] C. Hang, G. Huang, and V. V. Konotop, PT Symmetry with a System of Three-Level Atoms, Phys. Rev. Lett. **110**, 083604 (2013).
[12] P. Peng, W. Cao, C. Shen, W. Qu, J. Wen, L. Jiang, and Y. Xiao, Anti-parity-time symmetry with flying atoms, Nat. Phys. **12**, 1139 (2016).
[13] H. Xu, D. Mason, L. Jiang, and J. G. E. Harris, Topological energy transfer in an optomechanical system with exceptional points, Nature (London) **537**, 80 (2016).
[14] L. Feng, R. El-Ganainy, and L. Ge, Non-Hermitian photonics based on parity-time symmetry, Nat. Photonics **11**, 752 (2017).
[15] Ş. K. Özdemir, S. Rotter, F. Nori, and L. Yang, Parity-time symmetry and exceptional points in photonics, Nat. Mater. **18**, 783 (2019).
[16] W. Chen, Ş. K. Özdemir, G. Zhao, J. Wiersig, and L. Yang, Exceptional points enhance sensing in an optical microcavity, Nature (London) **548**, 192 (2017).
[17] L. Feng, Z. J. Wong, R.-M. Ma, Y. Wang, and X. Zhang, Single-mode laser by parity-time symmetry breaking, Science **346**, 972 (2014).
[18] H. Hodaei, M.-A. Miri, M. Heinrich, D. N. Christodoulides, and M. Khajavikhan, Parity-time-symmetric microring lasers, Science **346**, 975 (2014).
[19] P. Miao, Z. Zhang, J. Sun, W. Walasik, S. Longhi, N. M. Litchinitser, and L. Feng, Orbital angular momentum microlaser, Science **353**, 464 (2016).
[20] L. Feng, M. Ayache, J. Huang, Y.-L. Xu, M.-H. Lu, Y.-F. Chen, Y. Fainman, and A. Scherer, Nonreciprocal light propagation in a silicon photonic circuit, Science **333**, 729 (2011).
[21] S. Assawaworrarit, X. Yu, and S. Fan, Robust wireless power transfer using a nonlinear parity-time-symmetric circuit, Nature (London) **546**, 387 (2017).
[22] K. Kawabata, Y. Ashida, and M. Ueda, Information Retrieval and Criticality in Parity-Time-Symmetric Systems, Phys. Rev. Lett. **119**, 190401 (2017).
[23] C. W. Helstrom, Quantum detection and estimation theory, J. Stat. Phys. **1**, 231 (1969).
[24] C. A. Fuchs and J. van de Graaf, Cryptographic distinguishability measures for quantum-mechanical states, IEEE Trans. Inf. Theory **45**, 1216 (1999).
[25] H.-P. Breuer, E.-M. Laine, and J. Piilo, Measure for the Degree of Non-Markovian Behavior of Quantum Processes in Open Systems, Phys. Rev. Lett. **103**, 210401 (2009).
[26] H.-P. Breuer, E.-M. Laine, J. Piilo, and B. Vacchini, Colloquium: Non-Markovian dynamics in open quantum systems, Rev. Mod. Phys. **88**, 021002 (2016).
[27] T. Gao *et al.*, Observation of non-Hermitian degeneracies in a chaotic exciton-polariton billiard, Nature (London) **526**, 554 (2015).
[28] J. Li, A. K. Harter, J. Liu, L. de Melo, Y. N. Joglekar, and L. Luo, Observation of parity-time symmetry breaking transitions in a dissipative Floquet system of ultracold atoms, Nat. Commun. **10**, 855 (2019).
[29] Y. Wu, W. Liu, J. Geng, X. Song, X. Ye, C.-K. Duan, X. Rong, and J. Du, Observation of parity-time symmetry breaking in a single-spin system, Science **364**, 878 (2019).
[30] I. M. Georgescu, S. Ashhab, and F. Nori, Quantum simulation, Rev. Mod. Phys. **86**, 153 (2014).
[31] M. Huang, R.-K. Lee, L. Zhang, S.-M. Fei, and J. Wu, Simulating Broken PT-Symmetric Hamiltonian Systems by Weak Measurement, Phys. Rev. Lett. **123**, 080404 (2019).
[32] J.-S. Tang *et al.*, Experimental investigation of the no-signalling principle in parity-time symmetric theory using an open quantum system, Nat. Photonics **10**, 642 (2016).
[33] M. A. Nielsen and I. L. Chuang, *Quantum Computation and Quantum Information* (Cambridge University Press, Cambridge, England, 2000).
[34] M. B. Ruskai, Beyond strong subadditivity? Improved bounds on the contraction of generalized relative entropy, Rev. Math. Phys. **06**, 1147 (1994).
[35] For an open system, this property holds under the assumption that the system is uncorrelated with the environment initially, and the environment is independent with the system-state preparation.
[36] A. Gilchrist, N. K. Langford, and M. A. Nielsen, Distance measures to compare real and ideal quantum processes, Phys. Rev. A **71**, 062310 (2005).
[37] See Supplemental Material at http://link.aps.org/supplemental/10.1103/PhysRevLett.124.230402 for the experimental details and methods, the skew-eigenstate dynamical behaviors, and the conditions of conventional open quantum system, which includes Refs. [26,38–41].

[38] B.-G. Englert, C. Kurtsiefer, and H. Weinfurter, Universal unitary gate for single-photon two-qubit states, Phys. Rev. A **63**, 032303 (2001).

[39] D. F. V. James, P. G. Kwiat, W. J. Munro, and A. G. White, Measurement of qubits, Phys. Rev. A **64**, 052312 (2001).

[40] K. Kraus, *States, Effects, and Operations*, Lecture Notes in Physics (Springer, Berlin, 1983), Vol. 190.

[41] D. C. Brody and E.-M. Graefe, Mixed-State Evolution in the Presence of Gain and Loss, Phys. Rev. Lett. **109**, 230405 (2012).

[42] A. Mostafazadeh, Quantum mechanics of Klein-Gordon-type fields and quantum cosmology, Ann. Phys. (Amsterdam) **309**, 1 (2004).

[43] A. Mostafazadeh, A physical realization of the generalized PT-, C-, and *CPT*-symmetries and the position operator for Klein-Gordon fields, Int. J. Mod. Phys. A **21**, 2553 (2006).

[44] A. Mostafazadeh, Quantum Brachistochrone Problem and the Geometry of the State Space in Pseudo-Hermitian Quantum Mechanics, Phys. Rev. Lett. **99**, 130502 (2007).

[45] U. Günther and B. F. Samsonov, Naimark-Dilated PT-Symmetric Brachistochrone, Phys. Rev. Lett. **101**, 230404 (2008).

[46] Q. Li *et al.*, Experimental simulation of anti-parity-time symmetric Lorentz dynamics, Optica **6**, 67 (2019).

[47] A. Mostafazadeh, Pseudo-Hermitian representation of quantum mechanics, Int. J. Geom. Methods Mod. Phys. **7**, 1191 (2010).

[48] R. Grimaudo, A. S. M. de Castro, H. Nakazato, and A. Messina, Analytically solvable 2×2 PT-symmetry dynamics from su(1,1)-sym metry problems, Phys. Rev. A **99**, 052103 (2019).